

Ramsey Interference Fringes in Single Pulse Microwave Multiphoton Transitions

M. C. Baruch and T. F. Gallagher

Department of Physics, University of Virginia, Charlottesville, Virginia 22901

(Received 23 March 1992)

In microwave multiphoton transitions between Rydberg atoms driven by short microwave pulses we have observed that the rise and fall of the pulse are as important as the peak and together can produce readily visible interference in the transition probability. Furthermore, the transition probability vanishes for some tunings and can be suppressed if the ac Stark shift brings the two states into resonance at the peak of the microwave pulse with a large Rabi frequency.

PACS numbers: 32.80.Rm, 32.30.Bv

Theoretical work on multiphoton processes involving bound states, either by themselves [1] or as intermediate states en route to ionization [2], predicts several interesting features to be visible with spatially uniform radiation pulses. The effects arise from the fact that the intermediate state can shift into and out of multiphoton resonance due to the varying ac Stark shift of the levels during the pulse. Tang, Lyras, and Lambropoulos [2] have pointed out that Rabi oscillations should be manifested in the electron energy spectrum in resonantly enhanced multiphoton ionization, and Breuer, Dietz, and Holthaus [1] have pointed out that it should be possible to see Ramsey or Stueckelberg oscillations in the bound-bound transition probability as the peak intensity is varied. While the above effects are unlikely to be prominent in laser experiments, due to the spatial variation in the intensity at the laser focus, Freeman *et al.* [3] have observed resonantly enhanced photoelectron energy spectra from the temporal peak of the laser intensity.

Here we report the experimental observation of multiphoton transitions in K Rydberg atoms driven by short pulses of 9.3-GHz microwaves. In such experiments all the atoms are exposed to a microwave pulse of the same intensity [4,5], and we have explicitly observed the oscillations predicted by Breuer, Dietz, and Holthaus, which can be seen as a function of the frequency tuning, the pulse intensity, and the pulse width. Two other features emerge. First, at some detunings from resonance the transition probability vanishes. Second, if a long, > 30 ns, pulse shifts the states into resonance at the peak of the pulse, and there is a large Rabi frequency, the transition probability nearly vanishes, a counterintuitive result. We present our experimental results and explain them with a Floquet picture.

We have observed four photon transitions from the K $21s$ state to the $19,3$ state in combined static and microwave fields in the same direction. The $19,3$ state is the lowest-lying state of the $n=19$ Stark manifold. In this field regime each Stark state is a linear combination of $n=19$ $l \geq 3$ states. We follow the convention of Stoneman, Thomson, and Gallagher [4] of labeling K Stark states by (n,l) , where l is the angular momentum of the zero field state to which it is adiabatically connected. Figure 1 is an energy level diagram of the K $m=0$ states

as a function of a static electric field E_s . The $19,3$ state has a linear Stark shift, and the $21s$ state has a second-order shift. There is an avoided crossing at 304 V/cm, and the separation at the avoided crossing is $2V_0=320$ MHz, V_0 being the $21s$ - $19,3$ core coupling matrix element. The crossing field and $2V_0$ were measured by Stoneman, Janik, and Gallagher [6]. The $21s$ state is four 9.3-GHz photons below the $19,3$ state at a static field of $E_0=236.55$ V/cm. We have measured the dependence of the $21s$ - $19,3$ four-photon transition probability on the microwave pulse intensity, pulse length, and static tuning field in the vicinity of $E_s=237$ V/cm.

In the experiment a thermal beam of K atoms enters a microwave cavity through a hole in one sidewall and exits through a hole in the opposite sidewall. The atoms pass 5 mm above a septum in the cavity, which allows the application of a static field for tuning and a pulse for field ionization. The atoms are excited from the ground $4s$ state to the $4p$ state and finally to the $21s$ state by two col-

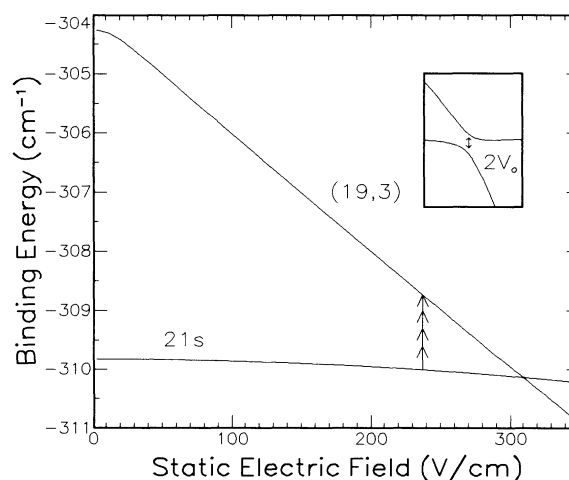


FIG. 1. K $21s$ and $19,3$ energy levels as a function of the static field E_s . There is an avoided crossing at 306 V/cm where the levels are separate by $2V_0=320$ MHz, as shown in the inset. The $21s$ state lies four 9.3-GHz photons below the $19,3$ state at $E_s=236.55$ V/cm. The $21s$ state is populated by the laser, the microwave pulse drives the $21s$ - $19,3$ transition, and the $19,3$ state is field ionized.

linear dye laser beams. About 100 ns after laser excitation a microwave pulse of chosen length and intensity is injected into the cavity, and 500 ns after the microwave pulse is turned off a high voltage pulse, which ionizes atoms in the 19,3 state but not in the 21s state, is applied to the septum. The ions formed are accelerated upward, and those ions created under a 0.3-mm-diam hole in the center of the top of the cavity escape and strike the microchannel plate detector. The detector signal is captured with a CAMAC-based gated integrator and recorded as the static field is swept over many shots of the laser.

The microwave cavity has inside dimensions 2.92 × 5.80 × 8.32 cm, and it contains a 2-mm-thick septum whose upper surface is 8 mm below the top of the cavity. We use the TE₁₀₅ mode which has an antinode at the center of the cavity. This mode has a resonance frequency of 9.255 GHz, a quality factor Q of 1600, and a time constant of 28 ns. The microwave power originates in a Hewlett-Packard (HP) 8350B sweep oscillator with an 83550 plug in. The microwaves pass through attenuators and a General Microwave 862B switch to a Hughes 1277H traveling wave tube amplifier. After the amplifier the microwaves pass through waveguide and then coaxial cable en route to the cavity. We can determine the microwave field to $\pm 10\%$.

All the data shown have been obtained by scanning the static field E_s so that the 21s-19,3 frequency interval varies from above to below 4×9.3 GHz. In Fig. 2 we

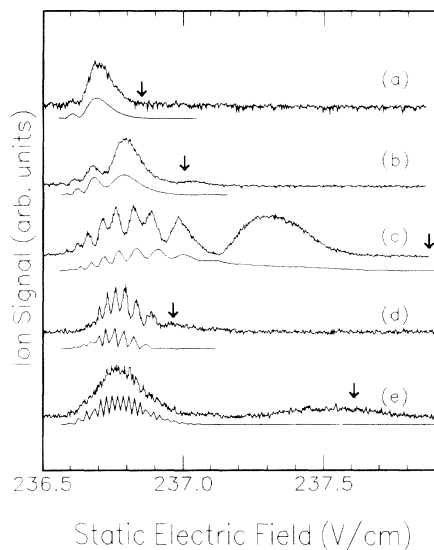


FIG. 2. The 19,3 signal as a function of the static tuning field for several pulse durations and peak amplitudes E_{pmw} (noisy trace). (a) 8-ns pulse and $E_{pmw} = 54$ V/cm, (b) 8-ns pulse and $E_{pmw} = 68$ V/cm, (c) 8-ns pulse and $E_{pmw} = 116$ V/cm, (d) 70-ns pulse and $E_{pmw} = 64$ V/cm, and (e) 70-ns pulse and $E_{pmw} = 104$ V/cm. Calculated spectra from Eq. (2) are shown (smooth traces), as well as arrows at the static fields at which E_{mw} brings the two levels into resonance.

show the population in the 19,3 state as the static tuning field is scanned for several peak microwave field strengths, E_{pmw} . It is important to remember that during the microwave pulse the microwave field amplitude E_{mw} rises from zero to E_{pmw} and then declines to zero. E_{mw} varies during the pulse, but E_{pmw} does not. In Figs. 2(a)-2(c) the injected pulse is 8 ns long, significantly shorter than the time constant of the cavity. With $E_{pmw} = 54$ V/cm, shown in Fig. 2(a), a single peak is observed at $E_s = 236.70$ V/cm. When E_{pmw} is raised to 69 V/cm [Fig. 2(b)] oscillations appear in the spectrum, starting at about $E_s = 236.55$ V/cm, the resonance position for $E_{mw} = 0$, and extending to higher static fields. As E_{pmw} is raised beyond 69 V/cm more oscillations appear, always on the high field side of $E_s = 236.55$ V/cm. It is also apparent, from the $E_{pmw} = 116$ V/cm scan of Fig. 2(c), that the higher static field peaks are both broader and farther apart. The arrows above each trace, for example, at a static field of 236.84 V/cm for Fig. 2(a), correspond to the positions of the resonance shifted by the ac Stark effect of the peak microwave field. As is evident in Fig. 2, the highest static field peak lies near this location.

With longer pulses the oscillations are more rapid, as can be seen by comparing Fig. 2(d), obtained with a 70-ns microwave pulse of $E_{pmw} = 64$ V/cm, to Fig. 2(b). In addition, comparing Figs. 2(c) and 2(e) we see that the transition probability is diminished at higher static fields.

The oscillations in Fig. 2 are the Ramsey or Stuckelberg oscillations predicted by Breuer, Dietz, and Holthaus [1]. They may be understood by using a Floquet description to remove the 9.3-GHz variation of the microwave field. Since the 19,3 state has a linear Stark effect, the effect of the added microwave field is to break it into a carrier and sideband states [4], each removed in energy from the carrier by an integral number of microwave photons. Specifically, the wave function of the 19,3 state is given by

$$\Psi(r,t) = \Psi(r) \sum_{n=-\infty}^{\infty} J_n(kE_{mw}/\omega) e^{-(W_k + n\omega)t}, \quad (1)$$

where W_k is the energy of the 19,3 state in the static field alone, k is its Stark coefficient, E_{mw} is the microwave field amplitude, ω is the microwave angular frequency, and $J_n(kE_{mw}/\omega)$ is a Bessel function [7]. The 21s state experiences only an ac Stark shift due to the microwave field. For E_s near 236.55 V/cm the coupling between the 21s and 19,3 states is entirely through the lower fourth sideband of the 19,3 state, and the coupling matrix element is $V_0 J_4(kE_{mw}/\omega)$, i.e., the core coupling matrix element multiplied by the fourth sideband's fractional amplitude, which depends on the microwave field through the Bessel function. We can consider an equivalent two-level problem in which the wave function is given by $\Psi(r,t) = A(t)\Psi_k(r) + B(t)\Psi_s(r)$, where Ψ_k and Ψ_s are the spatial wave functions of the 19,3 and 21s states. For a given static field the Schrödinger equation reduces to

$$\begin{pmatrix} W_k & V_{ks} \\ V_{sk} & W_s \end{pmatrix} \begin{pmatrix} A(t) \\ B(t) \end{pmatrix} = i \begin{pmatrix} dA/dt \\ dB/dt \end{pmatrix}, \quad (2)$$

where W_s and W_k are the Floquet energies and $V_{sk} = V_{ks} = V_0 J_4(kE_{mw}/\omega)$. For convenience we define zero Floquet energy as the energy at which the $21s$ state and the $19,3$ state minus four 9.3-GHz photons cross if there is no microwave field. With this convention, $W_s = -\alpha E_s(E_s - E_0) - \alpha E_{mw}^2/4$, and $W_k = -k(E_s - E_0)$. In frequency units the values of k and α are 506 MHz/(V/cm) and $0.1944 \text{ MHz}/(\text{V/cm})^2$ [4,8].

For constant microwave field amplitude and static field the Floquet energies are obtained by diagonalizing the Hamiltonian matrix of Eq. (2) [4]. In Fig. 3 we show the Floquet energies as a function of the microwave field amplitude for static fields of 236.7, 237.2, and 238.4 V/cm, for which W_s lies 69, 299, and 851 MHz above W_k when $E_{mw} = 0$. As shown by Fig. 3 the $21s$ energy decreases quadratically with E_{mw} due to the ac Stark shift. In Figs. 3(a)–3(c) there are avoided crossings of 12, 99, and 35 MHz, the differences coming from the different microwave fields at which they occur. The magnitude of the avoided crossing is the four-photon Rabi frequency between the two levels.

Since the microwave field amplitude changes slowly compared to the frequency, we can compute the effect of a pulse by explicitly including the time dependence of the energies and the coupling in Eq. (2) and numerically integrating it. This procedure gives results in reasonable agreement with the data, as shown in Fig. 2. It is more instructive, though, to consider a simple picture of the time evolution of the two levels along the energy levels of

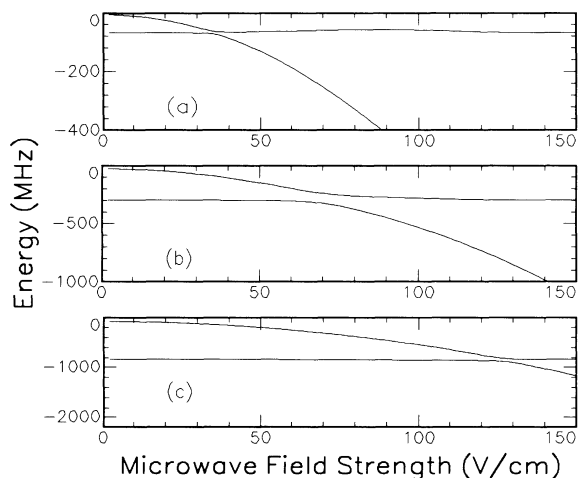


FIG. 3. The Floquet energies W_s and W_k , corresponding to the $21s$ and $19,3$ states, as functions of the microwave field E_{mw} for the static fields E_s of (a) 236.7 V/cm, (b) 237.2 V/cm, and (c) 238.4 V/cm. W_k is displaced from (a) to (c) by the linear $19,3$ static Stark shift, and W_s is displaced primarily by the ac Stark shift. The avoided crossing is 12, 99, and 35 MHz in (a), (b), and (c).

Fig. 3 during the pulse. Consider Fig. 3(a), relevant to the data shown in Fig. 2. As E_{mw} increases, an atom initially in the $21s$ state follows the $21s$ energy and will have a reasonable transition probability to the $19,3$ state only if E_{mw} reaches the avoided crossing at $E_{mw} = 38 \text{ V/cm}$. If E_{mw} goes beyond the avoided crossing and the crossing is traversed partially diabatically, a Landau-Zener transition occurs, and there are nonzero amplitudes in both levels. They evolve separately according to their energies and are recombined when the avoided crossing is traversed a second time on the falling edge of the pulse. The final $19,3$ amplitude is the sum of the transition amplitudes for the two traversals of the avoided crossing. Whether they add constructively or destructively depends on the phase difference Φ between the two levels accumulated between the two traversals of the avoided crossing. Explicitly, $\Phi = \int (W_k - W_s) dt$, integrated over the time between the two traversals. If $\Phi = 2\pi N$, where N is an integer, the amplitude addition is constructive, and if N is half integral it is destructive. Inspecting Fig. 3, we see that as the static tuning field is increased the energy of the $19,3$ state decreases, and the value of Φ decreases. Its maximum value occurs for $E_s = 236.55 \text{ V/cm}$, and $\Phi = 0$ when the two states come into resonance only at the peak of the microwave pulse.

Increasing either the peak microwave field amplitude or the pulse length increases Φ , and more peaks appear for the same scanning range of the static field.

With $E_{mw} = 104 \text{ V/cm}$ the two levels are brought into resonance at $E_s = 237.67 \text{ V/cm}$, where the Rabi frequency $2V_{sk} = 125 \text{ MHz}$, yet the signal is very small at $E_s = 237.67 \text{ V/cm}$ with the 70-ns pulse length of Fig. 2(e) in spite of the fact that $E_{pmw} = 104 \text{ V/cm}$. This case corresponds to Fig. 3(b). Because of the large Rabi frequency, or equivalently avoided crossing, the evolution from the initial $21s$ state to the high field and back again is almost completely adiabatic; no transition occurs. Note that in Fig. 4(c), also recorded with a 70-ns pulse, the transitions can again occur for higher microwave peak fields and larger static fields because the avoided crossings become smaller, as shown by Fig. 3(c), and the evolution in the pulse is no longer purely adiabatic.

In Figs. 4(a) and 4(b) we show scans taken with 8-ns pulses of higher peak amplitude. The transition probability extends to higher static fields, as expected. In addition, the overall signal and the oscillations become small at $E_s = 237.3 \text{ V/cm}$. Both decrease due to the avoided crossing's being transversed too slowly, and the oscillations decrease due to the asymmetry of the pulse as well. Finally, the transition probability vanishes at $E_s = 238.56 \text{ V/cm}$. For this static field the levels intersect at $E_{mw} = 135 \text{ V/cm}$, the field at which the first zero of $J_4(kE_{mw}/\omega)$ occurs. Consequently, the levels cross, the initial $21s$ state passes diabatically through the crossing, and no transition occurs, irrespective of the microwave field amplitude and pulse length, as shown by Figs. 4(b) and 4(d). Of course, for static fields in excess of 238

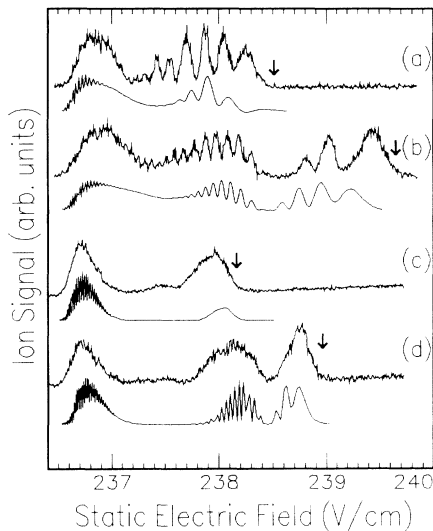


FIG. 4. The 19,3 signal as a function of the static tuning field for higher peak fields (noisy trace). (a) 8-ns pulse and $E_{\text{pmw}} = 141$ V/cm, (b) 8-ns pulse and $E_{\text{pmw}} = 178$ V/cm, (c) 70-ns pulse and $E_{\text{pmw}} = 127$ V/cm, and (d) 70-ns pulse and $E_{\text{pmw}} = 152$ V/cm. With higher peak fields the spectra extend to higher static fields than in Fig. 2. Note the decrease in the signal at $E_s = 237.4$ V/cm in (a) and (b). Note the abrupt reappearance of the signal at $E_s = 237.7$ V/cm in (c) and (d). In all cases the signal vanishes at $E_s = 238.4$ V/cm. Simulations from Eq. (2) are shown by smooth traces, and arrows show where the peak microwave field brings the two levels into resonance.

V/cm, the levels do not cross, and the transition again becomes possible, as shown by Figs. 4(b) and 4(d).

In conclusion, we have demonstrated experimentally that the rising and falling edges of the microwave pulse

are important and lead to readily visible interference. Furthermore, we have shown that transitions do not necessarily occur when the peak of the pulse brings the two states into exact resonance, and that a large Rabi frequency can actually inhibit transitions.

This work has been supported by the Air Force Office of Scientific Research. It is a pleasure to acknowledge useful suggestions of L. A. Bloomfield, M. D. Lindsay, and M. G. Renn.

Note added.—At the time of publication we learned of related work by Yoakum, Sirko, and Koch in which Stueckelberg oscillations were observed in the microwave excitation of helium triplet Rydberg atoms [9].

- [1] H. P. Breuer, K. Dietz, and M. Holthaus, *Z. Phys. D* **10**, 13 (1988).
- [2] X. Tang, A. Lyras, and P. Lambropoulos, *Phys. Rev. Lett.* **63**, 972 (1989).
- [3] R. R. Freeman, P. H. Bucksbaum, H. Milchberg, S. Darack, D. Schumacher, and M. E. Geusic, *Phys. Rev. Lett.* **59**, 1092 (1987).
- [4] R. C. Stoneman, D. S. Thomson, and T. F. Gallagher, *Phys. Rev. A* **37**, 1527 (1988).
- [5] W. van de Water, S. Yoakum, T. van Leeuwen, B. E. Sauer, L. Moorman, E. J. Galvez, D. R. Mariani, and P. M. Koch, *Phys. Rev. A* **42**, 572 (1990).
- [6] R. C. Stoneman, G. Janik, and T. F. Gallagher, *Phys. Rev. A* **34**, 2952 (1986).
- [7] S. H. Autler and C. H. Townes, *Phys. Rev.* **100**, 703 (1955).
- [8] J. Shirley, *Phys. Rev.* **138**, B979 (1965).
- [9] S. Yoakum, L. Sirko, and P. M. Koch, *Bull. Am. Phys. Soc.* **37**, 1105 (1992).